



Optimization of the Synthesis Conditions of N-Doped TiO₂ Nanoparticles

E. M. Bayan¹(✉), L. E. Pustovaya², Yu. A. Bayan¹, and T. G. Lupeiko¹

¹ Southern Federal University, Rostov-on-Don, Russia
ekbayan@sfedu.ru

² Don State Technical University, Rostov-on-Don, Russia

Abstract. A visible-light-active N-doped TiO₂ photocatalyst was prepared by the sol-gel method, employing urea as nitrogen source. Heat treatment was carried out in three different ways: low temperature, high temperature and hydrothermal without further calcinations. The effect of nitrogen addition (1–50 mol%) on the photocatalytic activity was also studied. The optimal conditions for the synthesis of materials with the highest photocatalytic activity have been established: hydrothermal synthesis for 24 h at 160 °C, 5 mol% N-doped TiO₂. The synthesized materials have a photocatalytic activity higher than that of Degussa P25 under UV light activation and higher than pure TiO₂ under visible light activation.

Keywords: Titanium dioxide · Anatase · Hydrothermal · Synthesis · Photocatalytic activity · Nitrogen

1 Introduction

Environmental pollution in the 21st century has acquired a global planetary scale. The sustainable development of modern civilization requires reducing the negative impact on natural ecosystems. New technologies and materials pollute the environment with contaminants, which requires further development of methods for cleaning the environment from them. Catalytic purification methods are currently considered the most promising, especially with the use of photoactivation [1, 2]. Semiconductor materials based on various oxides are used as photocatalysts. One of the promising materials for photocatalysis is titanium dioxide, since it is not only effective in water and air purification, but also chemically inert and low-cost. Pure TiO₂ has a large bandgap (3.2 eV) and is excited by ultraviolet irradiation. For a wide practical application, the photocatalyst should exhibit a bandgap suitable for excitation by visible light. An active study of the properties of this material led to the need to modify it to shift the region of the operating absorption frequency to the visible part of the spectrum and reduce the band gap [3, 4]. In this regard, many works investigate the effects of introducing cations of various metals into the structure of titanium dioxide. The authors report that the photocatalytic activity of metal doped materials increased significantly when irradiated with ultraviolet and visible radiation [5–8]. However, most of the introduced additives increase the toxicity of the catalyst material, making it unfavourable for the environment; therefore,

the effect of non-metallic additives on the properties of titanium dioxide is also being studied [9]. N-doped TiO₂ is of the greatest interest among all doped materials, while the form of existence of impurity nitrogen atoms and the nature of their influence on the properties of the material mainly depend on the prehistory of its production. Therefore, studying the influence of synthesis conditions on the final material properties is always an important task both from a practical and theoretical viewpoint. Thus, N-doped TiO₂ has attracted considerable attention as a photocatalyst, and rapid progress has been made in increasing the photocatalytic activity of titanium dioxide when irradiated with visible light. TiO₂ doped with nitrogen has a wide absorption in the visible region, which makes it possible to use a large part of the solar spectrum [10–12]. In this regard, a very large number of different methods for the synthesis of N-doped TiO₂ have recently appeared. Nanosized N-containing titanium dioxide materials can be obtained in two ways:

- (i) nitrogen is introduced into the finished titanium dioxide nanomaterial of known structure and phase (annealing of TiO₂ in an atmosphere of NH₃ or other N-containing compounds, impregnation with a N-containing precursor followed by annealing, etc.) [13–21];
- (ii) nitrogen is introduced into the system at one of the stages of precursor synthesis (sol–gel and hydrothermal method) [3, 22–26].

The choice of synthesis method determines the final properties of the material. The inclusion of a nitrogen atom in the TiO₂ lattice leads to the formation of a new average energy state, i.e., the N 2p band above the O 2p valence band, which ultimately reduces the TiO₂ band gap (to ~2.5 eV) and shifts the optical absorption to the region of visible light. Therefore, electrons can migrate from the valence band to the conduction band upon absorption of visible light, which leads to the activity of N-doped TiO₂ in visible light. [27–30]. In this regard, it is important to accumulate experimental data on the effect of the synthesis route on the photocatalytic properties of titanium dioxide modified with nitrogen.

In this work, we consider several strategies for the synthesis of N-doped TiO₂ and study the dependence of the photocatalytic activity of the obtained materials under both the UV- and visible light activation.

2 Experimental Part

2.1 Material Synthesis

The raw materials used in this study were titanium tetrachloride TiCl₄, urea (NH₂)₂CO, 5% ammonia solution NH₃, distilled water. All reagents were analytical reagents, commercially obtained and used without any further purification. All solutions were prepared using deionized water. At the first stage, the titanium hydroxide was synthesized by sol–gel method. Further, after washing it, a urea solution was added in the required proportions. The subsequent stages were carried out in accordance with the parameters shown in Table 1. Three heat treatment methods were used: low temperature (L), high temperature (H) and hydrothermal (HT).

Table 1 Materials composition and synthesis conditions

N-TiO ₂ - Nanomaterial number	Dopant concentration, mol%	Synthesis method	Calcination temperature, °C	Calcination time, hour	Structure	Crystallite size, nm
1	1	H	600	2	A	15
2	1	H	700	2	A	22
3	3	H	600	2	A	16
4	3	H	700	2	A	20
5	5	H	600	2	A	12
6	5	H	700	2	A	20
7	25	H	600	2	A	14
8	25	H	700	2	A	19
9	35	H	600	2	A	16
10	35	H	700	2	A	27
11	50	H	600	2	A	15
12	50	H	700	2	A	28
13	25	L	120	12	A	9
14	25	L	120	18	A	9
15	25	L	120	72	A	9
16	5	H	800	2	A	35
17	1	HT	160	24	A	9
18	1	HT	180	24	A	10
19	1	HT	200	24	A	10
20	3	HT	180	24	A	8
21	3	HT	200	12	A	9
22	3	HT	200	24	A	12
23	5	HT	160	24	A	7
24	5	HT	180	24	A	8
25	5	HT	200	24	A	10
26	25	HT	160	24	A	9
27	25	HT	180	24	A	10
28	25	HT	200	24	A	11
29	35	HT	160	24	A	10
30	35	HT	180	24	A	11
31	35	HT	200	24	A	12
32	50	HT	160	24	A	11
33	50	HT	180	24	A	11
34	50	HT	200	24	A	12
35	5	L	100	48	A	9

2.2 Materials Characterization

Thermogravimetric (TGA) and Differential Thermal Analysis (DTA) were carried out using a thermal analyzer (STA 449S/4G Jupiter Jupted) at a heating rate of 10 °C/min. The phase composition of the samples was studied by X-ray powder diffraction (XRD) analysis by using an ARL X'TRA, Thermo ARL (Switzerland), diffractometer equipped

with a high-intensity Cu-K α_1 irradiation ($\lambda = 1.540562 \text{ \AA}$) operated at 40 kV and 30 mA in the range of 20–60°. The morphological characteristics were analyzed with transmission electron microscopy (TEM) utilizing a TEM Tecnai G2 Spirit Bio TWIN microscope operating at 120 kV.

2.3 Photocatalyst Preparation

The photocatalytic activity of obtained materials was traced by monitoring of the discoloration of organic azo-dye—methylene blue (MB) in aqueous solution as described in the paper [12]. Experiments were carried out at room temperature under illumination of UV radiation (low-pressure mercury lam) or visible light (fluorescent light lamp) for different length of time. The MB concentration (C) was determined spectrophotometrically (spectrophotometer UNICO 1201). Each experiment was repeated at least three times. The photodegradation of MB was determined by C/C_0 , where C_0 and C are initial ($t = 0$) and variable concentrations of MB, respectively. Commercial catalyst Degussa P25 was used as a comparative sample.

3 Result and Discussion

3.1 DTA/TGA Measurements

To determine the optimal calcination temperatures, TG-DTA of titanium hydroxide, an intermediate product of the synthesis, was performed (Fig. 1). Several stages can be distinguished on the TG curve. In the temperature range up to 100 °C, there is a loss of mass (4.5%) due to the evaporation of adsorbed water. In this case, an endothermic peak is observed. At temperatures from 100 to 400 °C, a weight loss (4.5%) is observed, associated with the decomposition of titanium hydroxide to oxide. In the temperature range from 400 °C, the mass stabilizes, no obvious thermal effects are observed. Based on the data obtained for the heat treatment of materials, the calcination temperatures 600 and 700 °C were chosen.

3.2 XRD Patterns

The synthesized materials were studied by XRD. All samples before heat treatment were X-ray amorphous. It has been established that all materials crystallize in the anatase modification. Characteristic X-ray diffraction patterns of some materials calcined at 600 and 700 °C are shown in Fig. 2a and b, respectively. Traditionally, as the temperature increases, X-ray diffraction patterns show an increase in the intensity of the peaks and a decrease in their width, which indicates the crystallization of materials. From the width of the anatase (101) peak in X-ray diffraction patterns, the average sizes of crystallites were calculated, which amounted to 8–35 nm (Table 1). In this case, an increase in the heat treatment temperature leads to an increase in the particle size, which is obviously associated with crystallization processes. It can also be concluded that the particle size is practically independent of the amount of the introduced dopant.

The size and morphology of the synthesized materials were analyzed by transmission electron microscopy. A characteristic TEM photograph is shown in Fig. 3. It was

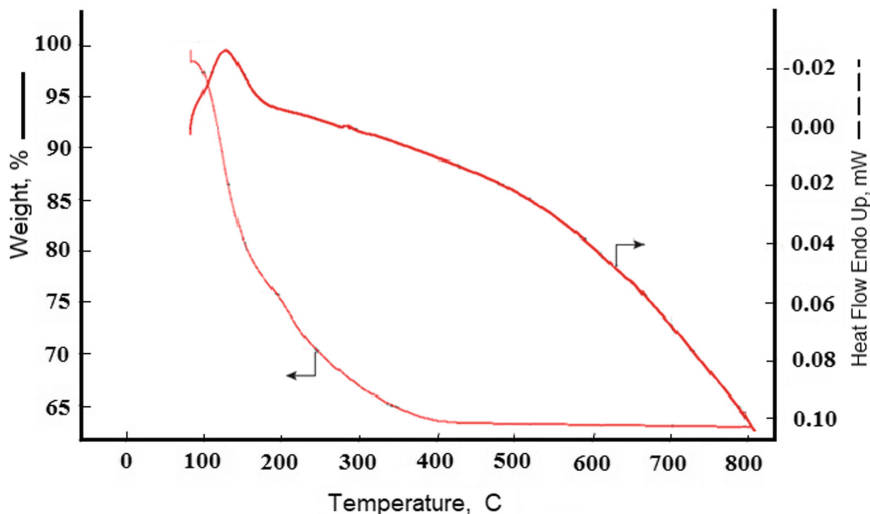


Fig. 1 Results of DTA-TG analysis of the titanium hydroxide with a content of 5 mol% nitrogen

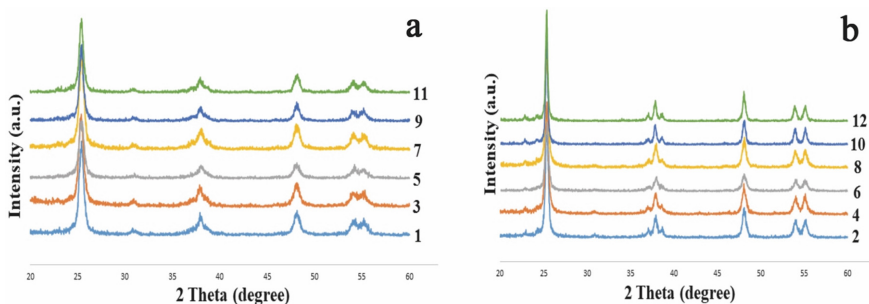


Fig. 2 XRD patterns of TiO₂-materials: (a) 1, 3, 5, 7, 9 and 11 calcined at 600 °C and (b) 2, 4, 6, 8, 10 and 12 calcined at 700 °C

found that the sol–gel method produced homogeneous materials with nanosized particles of predominantly spherical shape (Fig. 3a). N-TiO₂ materials synthesized by the hydrothermal method were composed of nanosized particles with a shape close to an oval (Fig. 3b). It is noted that materials are prone to agglomeration, which can be attributed both to the properties of the material itself, and to the features of sample preparation and the method of analysis in vacuum. According to transmission electron microscopy, the particle size is 10–22 nm for material 7. The data obtained correlate with the average crystallite size (the size of coherent scattering regions) obtained by calculation from the results of X-ray phase analysis.

The photocatalytic activity in aqueous solution of the obtained materials was studied using a model reaction of photodegradation of the organic dye methylene blue in aqueous suspensions of titanium dioxide under the action of UV radiation. A commercial catalyst Degussa P25, which is a mixture of two TiO₂ phases: anatase (86%) and rutile (14%),

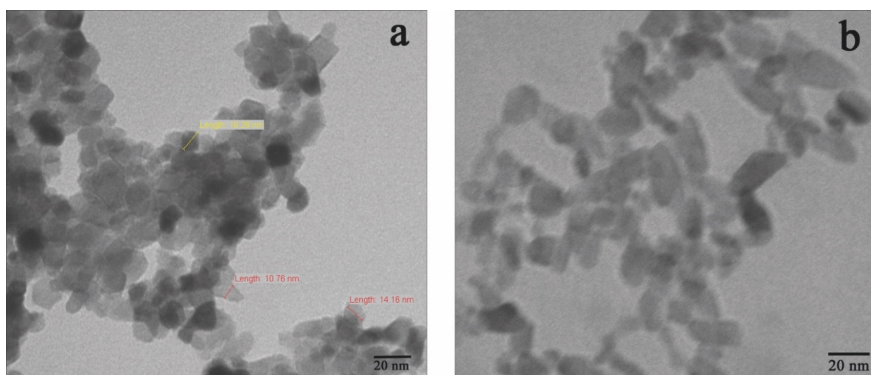


Fig. 3 TEM microphotographs of N-TiO₂ nanoparticles synthesized by low temperature sol-gel-material 7 (a) and hydrothermally treated-material 19 (b)

was used as a reference sample. The results of the photocatalytic activity of N-TiO₂ nanomaterials obtained by calcination at high temperatures are presented in the Fig. 5. Materials calcined at 600 °C (Fig. 4a) and 700 °C (Fig. 4b) showed photocatalytic activity under UV light activation almost twice that of a commercial catalyst Degussa P25. Among these materials, the N-TiO₂ nanomaterial containing 25 mol% of N exhibits the maximum activity. Similar photocatalytic activity to this sample is also exhibited by materials containing 35 or 50 mol% of N.

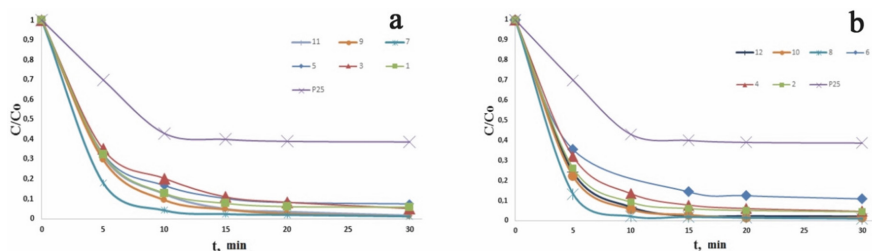


Fig. 4 Photodegradation of MB in presence of N-TiO₂ nanomaterials: (a) 1, 3, 5, 7, 9, 11 calcined at 600 °C and (b) 2, 4, 6, 8, 10, 12 calcined at 700 °C compared to Degussa P25 (P25) under UV light activation

The influence of the calcination temperature on the properties of N-TiO₂ nanomaterials has been studied. It has been established that with an increase in the calcination temperature, the photocatalytic activity also increases, reaching maximum values in the temperature range of 600–700 °C. This can be seen when comparing the graphs presented in Fig. 4.

The photocatalytic activity under UV light activation of the N-TiO₂ nanomaterials obtained by hydrothermal method for 24 h at different temperatures and containing different nitrogen concentrations is shown in Fig. 5. It is shown that all materials obtained by the hydrothermal method have a higher photocatalytic activity than commercial catalyst

Degussa P25. The photocatalytic activity of the best materials 23 obtained hydrothermally at 160 °C is comparable to materials 18, 20 at 180 °C and 21, 22, 25 at 200 °C. At the same time, a similar trend is observed in the purification of solutions from MB (Fig. 5a in comparison with Fig. 5b and c). However, it can be noted that materials with a high concentration of nitrogen decompose organic pollutants worse than materials with a content of 1, 3, 5 mol% nitrogen.

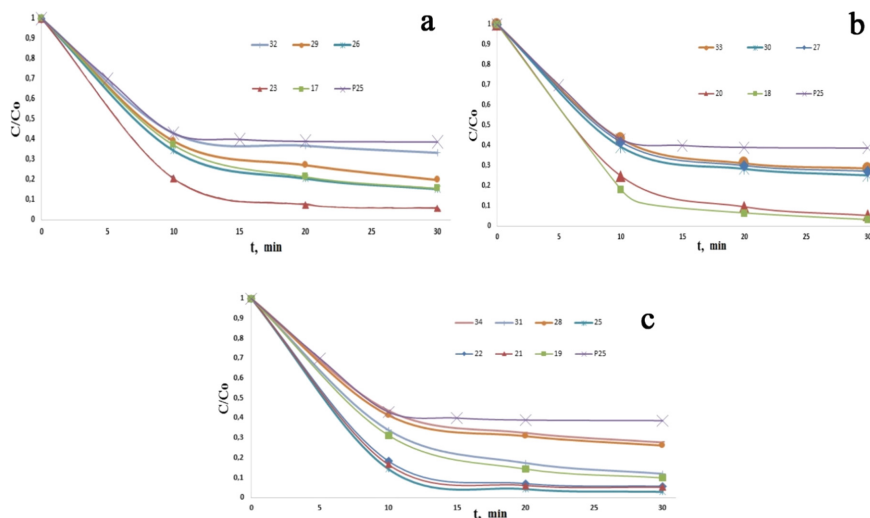


Fig. 5 The photodegradation of MB in presence of N-TiO₂ nanomaterials: (a) 17, 23, 26, 29, 32 ($T = 160$ °C); (b) 18, 20, 27, 30, 33 ($T = 180$ °C); (c) 19, 21, 22, 25, 28, 31, 34 ($T = 200$ °C) compared to Degussa P25 (P25) under UV light activation

The photocatalytic activity of N-TiO₂ nanomaterials under visible light activation was also studied in the reaction of methylene blue photodegradation. The results of the study are presented in the form of dependences of the proportions of photodegraded MB on the time of contact with the catalyst (Figs. 6 and 7). Materials 1 and 2, containing 1 mol% nitrogen, showed the highest photocatalytic activity among materials treated at high temperature (Fig. 6). Materials calcined at 700 °C show higher photocatalytic activity than materials heat treated at 600 °C. This is due to a decrease in the proportion of the amorphous phase and an increase in the crystallinity of the anatase modification.

The results of the photocatalytic activity of N-TiO₂ nanomaterials obtained by calcination at low temperatures are presented in Fig. 7.

The N-TiO₂ nanomaterials 35, thermally treated at 100 °C for 48 h, exhibits higher photocatalytic activity compared to materials 13–15, thermally treated at 120 °C for 12–72 h. Materials 14 and 15 exhibit similar photocatalytic activity. Thus, it can be assumed that “mild” heat treatment in combination with a small amount of nitrogen contributes to the formation of a microstructure that prevents bulk recombination, which in turn increases the quantum yield of the photodegradation reaction, that is consistent with the data described in paper [4].

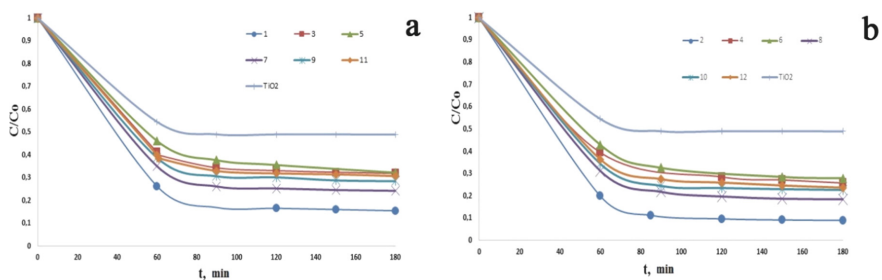


Fig. 6 Photodegradation of MB in presence of N-TiO₂ nanomaterials: (a) 1, 3, 5, 7, 9, 11; (b) 2, 4, 6, 8, 10, 12 compared to TiO₂ under visible light activation

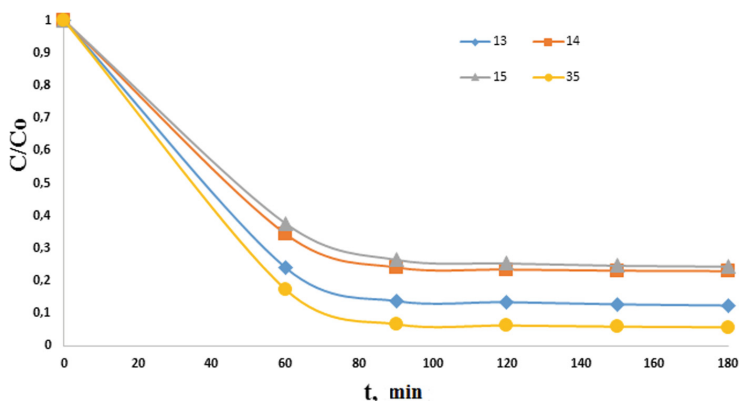


Fig. 7 Photodegradation of MB in presence of N-TiO₂ nanomaterials 13–15, 35 under visible light activation

The photocatalytic activity under visible light activation of the N-TiO₂ nanomaterials obtained by hydrothermal method for 24 h at different temperatures and containing different nitrogen concentrations is shown in Fig. 8. The N-TiO₂ nanomaterials obtained by the hydrothermal method show the closest and highest photocatalytic activity under visible light activation, except for materials with a content of 50 mol% nitrogen (material 32, 33 and 34).

Based on the presented data, it can be concluded that nitrogen doping of the materials promotes a shift in the absorption spectrum to the visible region of the solar spectrum and an increase in the photocatalytic activity of nanomaterials under visible light activation.

4 Conclusions

In this work, a comparative assessment of the thermal treatment conditions for the photocatalytic properties of N-doped TiO₂ nanoparticles under UV- or visible light activation is carried out. It is shown that nitrogen doping makes it possible to stabilize the catalytically active anatase modification of titanium (IV) oxide. The hydrothermal method makes it possible to obtain N-doped TiO₂ nanoparticles with the smallest particle

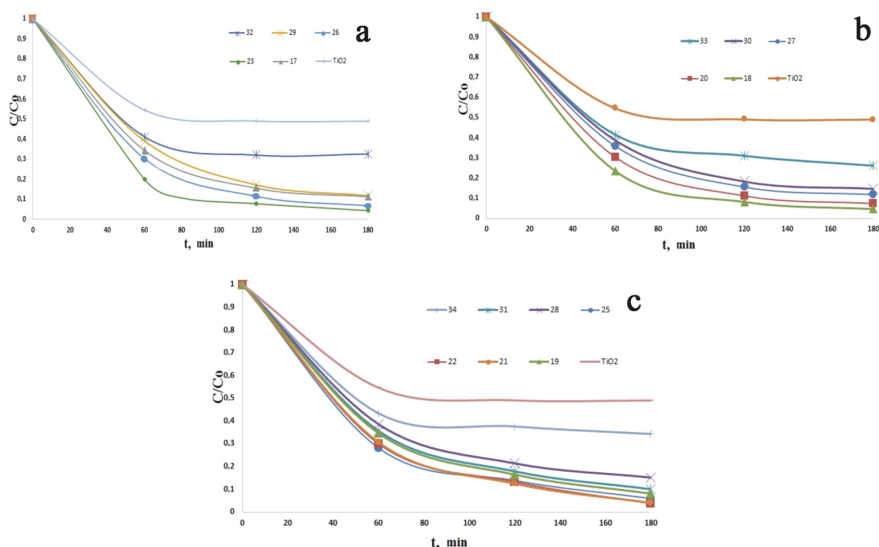


Fig. 8 Photodegradation of MB in presence of N-TiO₂ nanomaterials: (a) 17, 23, 26, 29, 32 ($T = 160\text{ }^{\circ}\text{C}$); (b) 18, 20, 27, 30, 33 ($T = 180\text{ }^{\circ}\text{C}$); (c) 19, 21, 22, 25, 28, 31, 34 ($T = 200\text{ }^{\circ}\text{C}$) compared to TiO₂ under visible light activation

size ($\sim 10\text{ nm}$), which ensures high quality of photocatalytic materials. The synthesized materials, when activated with UV light, show photocatalytic activity higher than that of the industrial commercial Degussa P25 catalyst. Materials with a nitrogen content of 1–5 mol% also have a high photocatalytic activity under visible light activation, which can significantly expand the possibilities of using this catalyst. The conditions for the synthesis of materials with the highest photocatalytic activity were established: hydrothermal synthesis for 24 h at $160\text{ }^{\circ}\text{C}$ with the introduction of 5 mol% nitrogen. It has been established that hydrothermal synthesis has advantages in terms of energy efficiency and environmental friendliness, because it is carried out under mild synthesis conditions in the absence of toxic organic solvents.

Acknowledgement. We thank the “Modern Microscopy” Center for Shared Use of Scientific Equipment, Southern Federal University, Rostov-on-Don, Russia, for allowing us to study the microstructure of the samples.

References

1. Fiorenza R, Di Mauro A, Cantarella M et al (2020) *Mater Sci Semicond Process* 112:105019
2. Bayan EM, Volkova MG, Pustovaya LE (2021) *Environ Technol Innov* 24:101822
3. Le TTT, Tran DT, Danh TH (2021) *Chem Phys* 545:111144
4. Shiwen D, Lian J, Zhang F (2022) *Trans Tianjin Univ* 28:33–52
5. Basavarajappa PS, Patil SB, Ganganagappa N et al (2020) *Int J Hydrogen Energy* 45(13):7764–7778

6. Varma KS, Tayade RJ, Shah KJ et al (2020) *Water-Energy Nexus* 3:46–61
7. Bayan EM, Lupeiko TG, Pustovaya LE (2018) *Russian. J Phys Chem B* 12(5):923–928
8. Bayan EM, Lupeiko TG, Kolupaeva EV, Pustovaya LE, Fedorenko AG (2017) *Russ J Phys Chem B* 11(4):600
9. Kong X, Peng Z, Jiang R et al (2020) *ACS Appl Nano Mater* 3(2):1373–1381
10. Ansari SA, Khan MM, Ansari MO, Cho MH (2016) *The Royal Society of Chemistry and the Centre National de la Recherche Scientifique. New J Chem* 40:3000–3009
11. Bayan EM, Lupeiko TG, Pustovaya LE (2019) *Russian J Phys Chem B* 13(12):383–388
12. Bayan EM et al (2017) *Nanotechnol Russ* 12(5):269–275
13. Zeng L, Lu Z, Li M et al (2016) *Appl Catal B* 183:308–316
14. Mangamma G, Ajikumar PK, Nithya R et al (2007) *J Phys D Appl Phys* 40:4597–4602
15. Li D, Huang H, Chen X et al (2007) *J Solid State Chem* 180:2630–2634
16. Peng F, Cai L, Yu H et al (2008) *J Solid State Chem* 181:130–136
17. Asahi R, Morikawa T, Ohwaki T, et al (2001) *Science* 293(5 528):269–271
18. Panepinto A, Cossement D, Snyders R (2021) *Appl Surf Sci* 541:148493
19. Huang J, Dou L, Li J et al (2021) *Wang J Hazard Mater* 403:123857
20. Suwannaruang T, Kamonsuangkasem K, Kidkhunthod P et al (2018) *Mater Res Bull* 105:265–276
21. Zhang MZ, Bando Y, Wada K (2001) *J Mater Sci Lett* 20:167–170
22. Sanchez-Martinez A, Ceballos-Sanchez O, Koop-Santa C et al (2018) *Ceram Int* 44(5):273–5283
23. Huang WC, Ting J-M (2017) *Ceram Int* 43(13):9992–9997
24. Bakre V, Tilve SG, Shirsat RN (2020) *Arab J Chem* 13(11):7637–7651. <https://www.sciencedirect.com/journal/arabian-journal-of-chemistry>
25. Li G, Zou B, Feng S et al (2020) *Phys B: Phys Condens Matter* 588:412184
26. Asahi R, Morikawa T, Irie H, Ohwaki T (2014) *Chem Rev* 114:9824–9852
27. Ansari SA, Khan MM, Ansari MO et al (2014) *RSC Adv* 4:16782–16791
28. Khan MM, Ansari SA, Pradhan D et al (2014) *Ind Eng Chem Res* 53:9754–9763
29. Dunnill CW, Parkin IP (2011) *Dalton Trans* 40:1635–1640
30. Zhang W, Zou L, Lewis R, Dionysio D (2014) *J Mater Sci Chem Eng* 2:28–40